Short communication

Effect of cathode composition on impedance rise in high-power lithium-ion cells: Long-term aging results

Ira Bloom [a,*], Benjamin G. Potter [a], Christopher S. Johnson [a], Kevin L. Gering [b], Jon P. Christophersen [b]

[a] *Electrochemical Technology Program, Argonne National Laboratory, 9700 South Cass Avenue, Argonne, IL 60439, USA*
[b] *Idaho National Laboratory, P.O. Box 1625, Idaho Falls, ID 83415, USA*

Abstract

Extended cycle- and calendar-life testing of lithium-ion cells has shown the effect of aluminum concentration in the cathode on the area-specific impedance versus time behavior of the cell. In cells with a $LiNi_{0.8}Co_{0.15}Al_{0.05}O_2$ (5% Al) cathode, the change in mechanism from $t^{1/2}$ to t occurred at about 35 weeks. Increasing the aluminum concentration to 10% ($LiNi_{0.8}Co_{0.1}Al_{0.1}O_2$) delayed the change for, approximately, an additional 30 weeks. The factors affecting the rate of increase during the parabolic and linear portions of the curve depended on cathode composition and particle size. The difference in the time it took for the change in mechanism was related to the cathode composition.
© 2005 Elsevier B.V. All rights reserved.

Keywords: Impedance rise; Lithium-ion; Cycle life; Calendar life

1. Introduction

In a previous paper, we reported the results from calendar- and cycle-life aging experiments using 1 Ah, 18650 lithium-ion cells [1]. These cells consisted of a $LiNi_{0.8}Co_{0.15}Al_{0.05}O_2$ (Group A) or $LiNi_{0.8}Co_{0.1}Al_{0.1}O_2$ (Group B) positive electrode (cathode), a MAG-10 graphite negative electrode (anode), and a 1.2 M $LiPF_6$ in EC/EMC (3:7 by wt.) electrolyte. The cells were tested for calendar- and cycle-life at 45 °C.

The discharge area-specific impedance (ASI) data displayed both chemistry- and test-dependence. The Group B cells displayed higher rates for ASI rise and power fade than the Group A cells. The time-dependence of the ASI of the Group A cells displayed two distinct kinetic regimes; the initial portion depended on $t^{1/2}$ and the final, on t. The change in time-dependence occurred at about 35 weeks. On the other hand, the ASI of the Group B cells depended on $t^{1/2}$ only. The rate of increase was higher in the cycle life cells than in the calendar-life cells, regardless of cell chemistry. Since the only difference between these groups was the cathode, the ASI behavior was attributed to the difference in Al (and Co) content.

Testing continued on three Group B cells (one calendar-life and two cycle-life) from the above study for about an additional 52–60 weeks. We found that the ASI behavior of these remaining cells mimicked that found in the Group A cells, but the change in the ASI versus time behavior occurred later in cell life.

2. Experimental

Detailed information regarding the cell construction is given in Ref. [1]. The cell chemistry for Group A is given in Table 1. As stated above, Groups A and B differed in the composition of the cathode; that of Group B was $LiNi_{0.8}Co_{0.1}Al_{0.1}O_2$. The nominal capacity of the Group A cells was 1 Ah, while that of the Group B cells was 0.8 Ah. The cells had an average active area of 846.3 cm^2. The calendar-life cells were tested at Argonne

---

* Corresponding author. Tel.: +1 630 252 4516; fax: +1 630 252 4176.
  E-mail address: bloom@cmt.anl.gov (I. Bloom).

Table 1
Cell chemistry

Cathode electrode	Anode electrode
8 wt.% PVDF binder (Kureha KF-1100)	8 wt.% PVDF binder (Kureha #C)
4 wt.% SFG-6 graphite (Timical)	92 wt.% MAG-10 (Hitachi)
4 wt.% carbon black (Chevron)	4.9 mg/cm^2 loading density
84 wt.% LiNi$_{0.8}$Co$_{0.1}$Al$_{0.1}$O$_2$ (D-50 = 10.3 μm)	35 μm-thick coating/side
8 mg/cm^2 loading density	18 μm-thick Cu current collector
35 μm-thick coating/side	
30 μm-thick Al current collector	
Electrolyte	Separator
1.2-M LiPF$_6$ in EC/EMC (3:7 by wt)	25 μm-thick Celgard 2325 separator

National Laboratory; the cycle-life cells, at Idaho National Laboratory.

The testing protocols and methods are described in Refs. [1–3]. The cells were tested for cycle and calendar life at 60% SOC, corresponding to 3.723 and 3.741 V for Groups A and B, respectively. The aging temperature was 45 °C.

The cells were characterized in terms of their ASI values before the tests began by using the hybrid pulse-power characterization test at the low current value (L-HPPC) and of their C/1 capacities [1–3]. Here, the L-HPPC test was scaled to a 5 C discharge current and a 3.75 C regen current. After 4 weeks at temperature, the cells were cooled to 25 °C and reference performance tests (RPTs) were performed. The RPTs consisted of portions of the characterization tests, including the C/1 capacity and L-HPPC tests. The cells were then heated back to the aging temperature; see Refs. [1,3] for more information.

The derived C/1 capacity and L-HPPC impedance values from the two test labs were pooled and analyzed for trends. The impedance at 60% SOC from the L-HPPC test was selected for analysis because it corresponds to the nominal SOC anticipated for hybrid electric vehicle operation. The value at 60% SOC was approximated by linear interpolation using the FORECAST function in Microsoft EXCEL.

The nature of the time-dependence of the impedance was determined by curve fitting. For simple equations, such as $at^{1/2} + d$, where t is the time, and a and d are the constants, the data were fitted by using the LINEST function in EXCEL. For more complex equations, such as $at^{1/2} + c(t - t_0) + d$, where t is the time and a, c, d, and t_0 are the constants ($c = 0$ when $t < t_0$), the data were fitted by using the nonlinear regression function in Jandel SigmaStat. All values of the regression coefficient, r^2, were 0.97 or better.

The analytic form of the equation, $at^{1/2} + c(t - t_0) + d$, can be converted into rate expressions for the two mechanisms that govern the increase of impedance. The a parameter is related to the rate constant of the parabolic portion of the entire process, and the c parameter is related to the linear portion of the reaction process. The d parameter is the average

initial value of the ASI, and t_0 represents the average time at which the change in mechanism occurs.

3. Results

In our earlier paper, the discharge ASI data from the Group B calendar- and cycle-life cells were fitted to $t^{1/2}$ equations with high values of r^2 [1]. These fits were based on data from 60 and 56 weeks of testing for the calendar- and cycle-life cells, respectively.

As expected, the ASI of the Group B cells continued to increase with aging time. A plot of the ASI values at 60% SOC versus time for Group B is given in Fig. 1. Also included in Fig. 1 are fits of the data to $t^{1/2}$. Even though the value of the regression coefficient is acceptable (r^2 ~0.98), the fitted curve has significant deviations from the experimental data. At intermediate times, ~20–80 weeks, the fits tend to overestimate the data. The deviations are more obvious at long aging time, >80 weeks. At these long times, the fits tend to underestimate the ASI values. Together, these observations indicate that the $t^{1/2}$ equation may not be the best way to represent the data.

The fact that the fits underestimate the data suggests that there may be a change of mechanism occurring during the later stages of the aging process as seen in the Group A cells [1]. Fitting the Group B data to the non-linear equation, ASI $= at^{1/2} + c(t - t_0) + d$, yielded significantly better-quality fits. The nonlinear fits to the data, as well as those from Group A, are given in Fig. 2. The fitting parameters and values of the regression coefficients for the Group B cell are given in Table 2, along with those from Group A. The values of the regression coefficients, r^2, are now 0.99–1.00 for the Group B cells. Indeed, graphically speaking, the nonlinear representation of the data is better; there are no large regions of under- or over-estimation like those seen in Fig. 1.

From the data in Table 2, several other observations can be made. The values of t_0 for Group B are larger than those
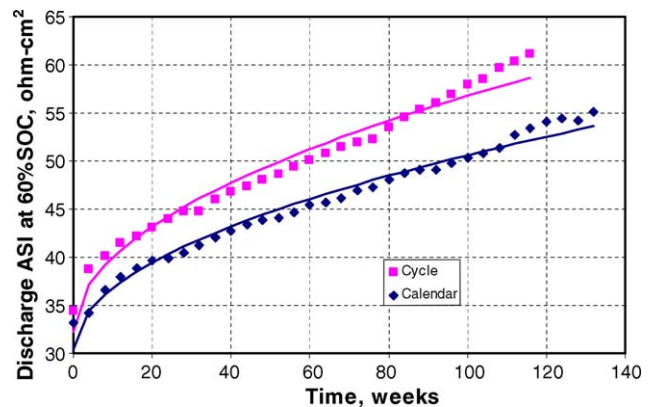

Fig. 1. Discharge ASI at 60% SOC for Group B cells at long aging times with fits to $t^{1/2}$ equations. There are deviations from the data in the time interval of ~20–80 weeks, for example, for the cycle-life fit. Here, the fit overestimates the ASI.
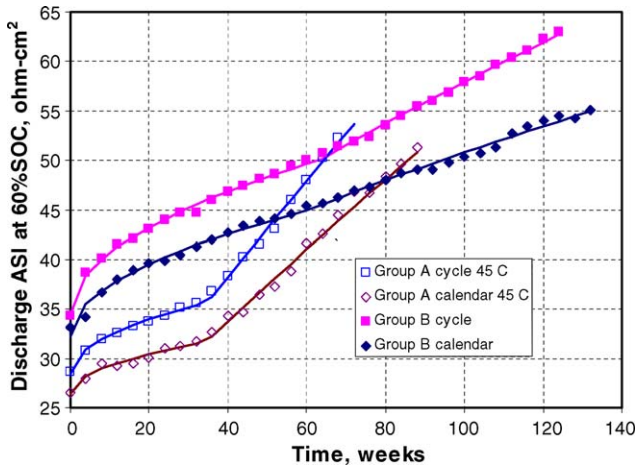
Fig. 2. Discharge ASI at 60% SOC vs. time for Groups A and B. The experimental data are represented as markers. The break in the curves is obvious for Group A and is subtle for Group B.

for Group A. The larger values indicate that the change from the $t^{1/2}$ mechanism to that dependent on t occurs at a later stage in cell life. The values of c are the reverse; that is, Group A's values are larger than Group B's. The value of a is larger (in a given test type) for Group B than for Group A. Additionally, the values of a and c for the Group B cycle-life cells are greater than those from the Group B calendar-life cells, indicating that cycling exacerbates ASI growth. The same trend is seen in the data from Group A.

Further evidence of the change in mechanism was found in the dependence of the $C/1$ capacity versus time. As expected, since the $C/1$ capacity is affected by the impedance of the cell due to the high discharge rate, the behavior of the $C/1$ capacity with time is the same as that observed in the ASI for both cell groups. This is shown in Fig. 3a and b.

Curve fitting using the same equation as that for the ASI values shows that the $C/1$ capacity values can also be fitted with values of r^2 greater than or equal to 0.97. The fits are also shown in Fig. 3a and b and the fitting parameters are given in Table 3. Indeed, general observations can be made about the absolute values of the data in Table 3 similar to those made for Table 2. The values of t_0 are sensitive to the composition of the cathode, with that of Group B being larger than those of Group A. The values of t_0 indicate that there is essentially no sensitivity to the test type in Groups A or B; the values of t_0 are not statistically different. Additionally, the values of t_0 for both the ASI and capacity fits are within a standard error
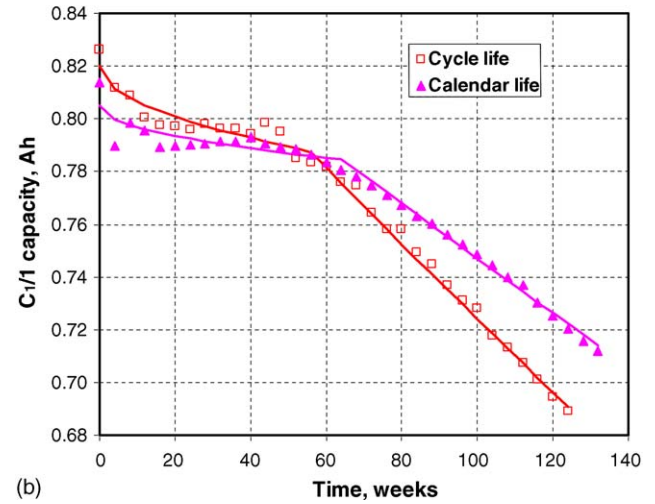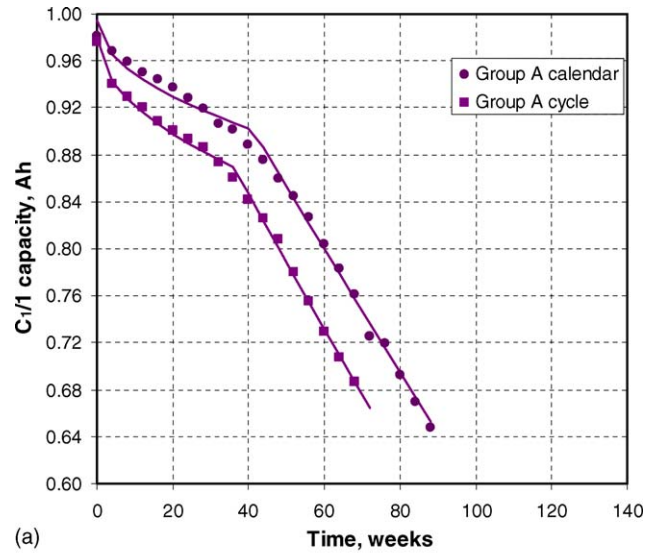

Fig. 3. (a) $C/1$ capacity of Group A cells with time. The trend shown in the curves mimics that found in Fig. 2. (b) $C/1$ capacity of Group B cells with time. The trend shown in the curves mimics that found in Fig. 2.

of each other for a given test type and cell chemistry, so that the two independent measurements are consistent with each other.

Within a group, the absolute values of a and c reflect the additional stress that cycling imposes on the cell; the cycle-life cells have larger values of these parameters. Interestingly, the values of these parameters change (for a given test type)

Table 2

Values of a, c, d, t_0, and r^2 for fits of ASI vs. time data shown in Fig. 2 and for the Group A cells from Ref. [1]

	Values				r^2	S.E.[a]			
	a	c	d	t_0		a	C	d	t_0
Group A, cycle life, 45 °C	1.23	0.40	28.46	35.15	1.00	0.08	0.01	0.34	0.90
Group A, calendar life, 45 °C	0.89	0.30	26.44	34.48	0.99	0.10	0.01	0.39	1.39
Group B, cycle life, 45 °C	1.96	0.11	34.45	63.45	1.00	0.04	<0.01	0.20	1.83
Group B, calendar life, 45 °C	1.64	0.05	32.16	59.70	0.99	0.06	0.01	0.30	5.34

[a] Standard error.

Table 3
Values of a, c, d, t_0, and r^2 for fits of $C/1$ capacity vs. time data shown in Fig. 3a and b

	Values				r^2	S.E.			
	a	c	d	t_0		a	C	d	t_0
Group A, cycle, life 45 °C	-1.73×10^{-3}	-4.93×10^{-3}	0.98	34.79	0.99	8.05×10^{-4}	1.44×10^{-4}	3.22×10^{-3}	3.13
Group A, calendar life, 45 °C	-1.33×10^{-3}	-4.27×10^{-3}	0.99	38.96	0.99	1.37×10^{-3}	2.03×10^{-4}	5.82×10^{-3}	1.43
Group B, cycle life, 45 °C	-4.29×10^{-3}	-1.19×10^{-3}	0.82	55.43	0.99	4.47×10^{-4}	4.42×10^{-5}	2.28×10^{-3}	1.81
Group B, calendar life, 45 °C	-2.56×10^{-3}	-9.12×10^{-4}	0.81	64.52	0.98	3.67×10^{-4}	4.44×10^{-5}	2.08×10^{-3}	2.32

by a factor of ∼2–5 when the composition of the cathode changes, with the values from Group B being lower than those from Group A.

4. Discussion

Since the major difference between the groups of cells is the composition of the cathode, it is reasonable to infer that initial values and the changes in the ASI are due to that electrode. Thus, the effects of Al concentration on the structural, electronic, and thermodynamic properties of the cathode material should be included in this discussion. Conceptually, both cathode materials can be thought of as solid solutions of $LiAlO_2$ and cobalt-doped $LiNiO_2$. $LiNiO_2$ is isostructural with $LiCoO_2$ (see Fig. 4a for crystal structure [4]); the trends observed in one should be applicable to the other regarding structural changes with Al content. The work of Alcántara et al. [5–7] and Lee et al. [8] has shown that the location and coordination of Al within the $LiCoO_2$ lattice is concentration-dependent. At low concentrations (ca. 3%), Al prefers a tetrahedral site in the lattice, which is between the
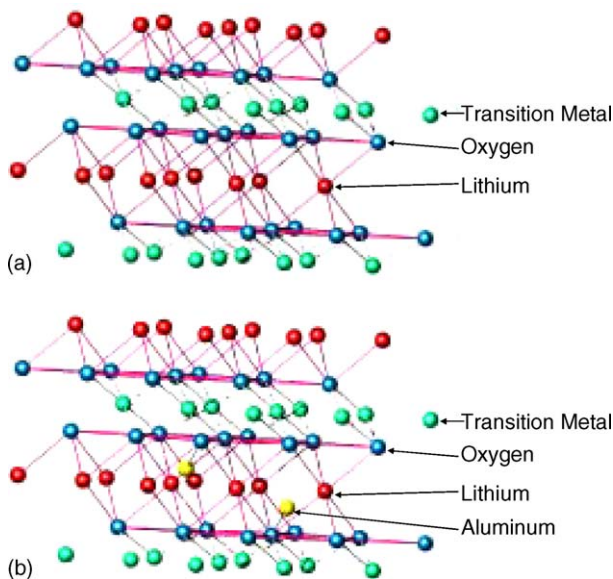

Fig. 4. (a) Crystal structure of parent compound, $LiCoO_2$ (atomic positions from Ref. [4]). (b) Crystal structure of $Li(Co,Al)O_2$ showing there are two tetrahedral sites between the Co and Li layers that Al can occupy [6,7]. This figure does not show the other structural changes caused by the presence of Al on the tetrahedral site, such as perturbation of the lithium layer.

lithium layer and cobalt oxide layer (see Fig. 4b); at higher concentrations (ca. 20% to 70%), Al prefers the octahedral sites (Co sites).

Aluminum substitution in the $LiNiO_2$ lattice is also expected to affect the electronic and ionic conductivity of the host material. The question is, which type of conductivity would be affected more? If Al were to substitute on the Ni site, then there would be a decrease in the number of available valence electrons, since Al^{3+} cannot be oxidized, and there would be fewer Ni^{3+} centers. Even though there are fewer of them, electrons still may be able to migrate fairly freely into and out of the structure, possibly decreasing the electronic conductivity slightly. However, relatively little effect on Li^+ diffusion in the lithium layer would be expected. If Al were to occupy the tetrahedral site, Al near the Li layer would be expected to impede the rapid diffusion of Li^+ in and out of the lattice due to lattice distortion, electrostatic interactions, etc. Thus, the ionic conductivity would be expected to show a greater effect. The initial ASI values are consistent with this concept; the initial ASI values of Group B exceed those of Group A.

$LiAlO_2$ is a more thermodynamically stable material than cobalt-doped $LiNiO_2$. One would expect the thermodynamic stability of the solid solution to be proportional to the concentration of $LiAlO_2$. When $LiAlO_2$ is incorporated into the cathode material, it also limits the amount of electrochemically active lithium that can be removed from the material. Using these concepts, one would expect the Group B cathode, with its higher Al concentration, to be less reactive. From the data, there is an apparent contradiction between the values of a and the expected relative thermodynamic stability of Group A versus Group B. That is, the initial parabolic rate, $1/2 \, at^{-1/2}$, is higher for Group B than for Group A. However, when the location of Al in the structure is considered, it is not unreasonable to expect that growth of a resistive surface layer [9] would influence the diffusion of Li^+ ions in the high-Al-containing structure (Group B) to a greater extent.

Another possibility is that the higher concentration of Al in Group B accelerated the initial degradation of PF_6^- into PF_5 and F^-. The result of this degradation would be a greater rate of LiF deposition on the cathode early in its life. The result of the greater rate of deposition would be an increase in the rate of ASI growth, which is initially parabolic.

Later in cell life, there is a change in reaction kinetic rate law from parabolic to linear. That is, the reaction mechanism may change from diffusion control to surface reaction control.

Assuming that the surface reaction mechanism involves the evolution of oxygen (due to Ni^{4+} and/or Ni^{3+} reactivity), the time until the change and the degree of the change are related to the concentration of Al. If the concentration of Al is high, it should take a longer time for oxygen evolution to begin with the more stable material (less $Ni^{3+/4+}$ present). Also, the more stable material would be expected to evolve oxygen at a slower rate. These hypotheses are consistent with the values of t_0 and c; the more stable Group B material has a larger value of t_0 and a smaller value of c than the Group A material.

The bulk of the ASI increase seems to be confined to the cathode. The ASI increase may depend not only on the reactions that occur during the useful life of the battery, but also on what reactions occur during materials synthesis. Thus, the causes of ASI increase and the factors affecting it are quite complex and are the subject of much research [10].

Indeed, the reactions which are sensitive to the concentration of Al affect $C/1$ capacity and capacity loss. Early in life, as mentioned previously, the capacity tends to be lower with high Al content, but the rate of capacity fade decreases with increasing Al content. Thus, the effect of Al is complex.

5. Conclusions

Extended cycle- and calendar-life testing of lithium-ion cells has shown the effect of aluminum concentration in the cathode on the ASI versus time behavior of the cell. In cells with 5% Al in the cathode, the change in mechanism from $t^{1/2}$ to t occurred at about 35 weeks. Increasing the aluminum concentration to 10% delayed the change for about an additional 30 weeks. The factors affecting the rate of increase during the parabolic and linear portions of the curve depended on cathode composition. The difference in the time it took for the change in mechanism was also related to the cathode composition.

The results presented herein suggest that the presence of aluminum in lithiated cathode material plays a mixed role by accelerating early life impedance growth while stabilizing the rate of capacity loss over time. This scenario does not lend itself to producing cells well suited for high power applications (e.g., HEVs). However, there are a multitude of other applications requiring low to moderate power performance and long life that could be well served by Group B (or like) cells. Studies involving the variation of aluminum content in cathode materials could help optimize this parameter for a chosen set of performance criteria.

Acknowledgments

References

[1] I. Bloom, S.A. Jones, V.S. Battaglia, G.L. Henriksen, J.P. Christophersen, R.B. Wright, C.D. Ho, J.R. Belt, C.G. Motloch, J. Power Sources 124 (2003) 538.

[2] PNGV Battery Test Manual, DOE/ID-10597, Rev. 3, US Department of Energy, February 2001.

[3] PNGV Test Plan for Advanced Technology Development Gen 2 Lithium-Ion Cells, EHV-TP-121, Rev. 6, October 5, 2001.

[4] M. Holzapfel, C. Haak, A. Ott, J. Solid State Chem. 156 (1999) 470.

[5] R. Alcántara, P. Lavela, P.L. Relaño, J.L. Tirado, E. Zhecheva, R. Stoyanova, Inorg. Chem. 37 (1998) 264.

[6] R. Stoyanova, E. Zhecheva, E. Kuzmanova, R. Alcántara, P. Lavela, J.L. Tirado, Solid State Ionics 128 (2000) 1.

[7] E. Gaudin, F. Taulelle, R. Stoyanova, E. Zhecheva, R. Alcántara, P. Lavela, J.L. Tirado, J. Phys. Chem. B 105 (2001) 8081.

[8] Y. Lee, A.J. Woo, K.-S. Han, K.S. Ryu, D. Sohn, D. Kim, H. Lee, Electrochemica Acta 50 (2004) 491.

[9] The nature of the surface layer on the positive material is the subject of much debate. There is evidence that the nature of the layer depends on the oxide, electrolyte, and salt. A. Würsig, H. Buqa, M. Holzapfel, F. Krumeich, P. Novák, Electrochem. Solid State Lett. 8 (2005) A34.

[10] D.P. Abraham, Personal communication (2005).